catalysts

MDPI

Article

Organocatalysts for the Synthesis of Cyclic Carbonates under the Conditions of Ambient Temperature and Atmospheric CO_2 Pressure

Yeongju Seong †, Sanghun Lee †, Seungyeon Cho, Yoseph Kim * and Youngjo Kim *

Department of Chemistry, Chungbuk National University, Cheongju 28644, Chungbuk, Republic of Korea
* Correspondence: armadajo@gmail.com (Y.K.); ykim@chungbuk.ac.kr (Y.K.); Tel.: +82-43-261-3395 (Youngjo Kim)
† These authors contributed equally to this work.

Abstract: 2–(1*H*–1,2,4–Triazol–3–yl)phenol (**CAT–1**) was used as an organocatalyst for the coupling reaction of CO_2 and epoxides at an ambient temperature and atmospheric CO_2 pressure (1 bar). This compound has a structure in which a hydrogen bond donor, a hydrogen bond acceptor, and another hydrogen bond donor are adjacent in sequence in a molecule. The binary catalytic system of **CAT–1**/*n*Bu_4NI showed TON = 19.2 and TOF = 1.60 h^{-1} under 1 bar CO_2 at room temperature within 12 h using 2–butyloxirane. Surprisingly, the activity of **CAT–1**, in which phenol and 1*H*–1,2,4–triazole are chemically linked, showed a much greater synergistic effect than when simply mixing the same amount of phenol and 1*H*–1,2,4–triazole under the same reaction conditions. In addition, our system showed a broad terminal and internal epoxide substrate scope.

Keywords: organocatalysts; ambient conditions; cyclic carbonates; carbon dioxide; epoxides

Citation: Seong, Y.; Lee, S.; Cho, S.; Kim, Y.; Kim, Y. Organocatalysts for the Synthesis of Cyclic Carbonates under the Conditions of Ambient Temperature and Atmospheric CO_2 Pressure. *Catalysts* **2024**, *14*, 90. https://doi.org/10.3390/catal14010090

Academic Editors: Eun Duck Park and Antonio Monopoli

Received: 31 December 2023
Revised: 15 January 2024
Accepted: 16 January 2024
Published: 22 January 2024

1. Introduction

The cycloaddition of CO_2 and epoxides yielding cyclic carbonates, which are used as aprotic polar solvents, electrolytes for lithium–ion batteries, monomers for polymerization, and pharmaceutical intermediates, is one of the most important reactions, alongside the transformation of CO_2 as a C1 feedstock due to its atom economy and broad applicability [1,2]. To date, numerous catalytic systems for the synthesis of CO_2-based cyclic carbonates, including various types of metal- and organic-based catalysts, have been reported in the literature [3–5]. Although organocatalysts have many advantages in terms of cost, toxicity, eco-friendliness, and accessibility, they generally require high reaction temperatures (>100 °C), high CO_2 pressures (>10 bar), and high catalyst loadings (>5 mol%) for efficient conversion, and also these reaction conditions are more stringent than those required by metal-based catalysts. To date, several active organocatalysts for this coupling reaction under mild conditions have been reported in the literature [6–8]; however, the development of efficient organocatalysts capable of operating at an ambient temperature and atmospheric CO_2 pressure is quite difficult, and only a few examples are known [9–16].

Pairs of hydrogen–bond donors (HBDs) as organocatalysts and nucleophiles as cocatalysts are well-known catalytic systems for the synthesis of CO_2-based cyclic carbonates under mild conditions [17–19]. Phenol and its derivatives are among the most extensively investigated examples of HBDs because they can easily be modified to include substituents that have steric and electronic effects on the other five carbon atoms in the phenyl ring [20–25]. In addition, HBDs with more than two vicinal –OH groups, which can interact synergistically with the O atom of the epoxide through H–bonds, exhibit higher activities than HBDs with non-vicinal –OH groups or only one –OH group [21–25]. To the best of our knowledge, HBDs with two different vicinal groups, specifically –OH and –NH groups, have never been used as catalysts for CO_2/epoxide coupling reactions, even

though organocatalysts with two vicinal NH groups have recently been reported [26,27]. Furthermore, pyridine-like N atoms in the catalyst can activate CO_2 to afford carbamate intermediates during the catalytic cycle [15]. Thus, designing simple organocatalysts with cooperative H-bond sites and multiple CO_2-activating sites located close to or adjacent to each other within a single molecule is highly desirable. As shown in Figure 1, we demonstrate that 2–(1*H*–1,2,4–triazol–3–yl)phenol (**CAT–1**) with cooperative H-bonds from the vicinal –OH group and –NH group and with pyridine-like N atoms that can activate CO_2 in a single molecule can be a practical alternative to metal catalysts for the synthesis of CO_2-based cyclic carbonates at an ambient temperature and atmospheric CO_2 pressure.

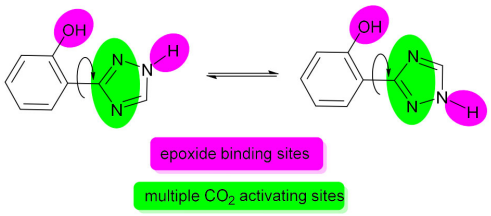

Figure 1. 2–(1*H*–1,2,4–Triazol–3–yl)phenol as a catalyst for the fixation of CO_2 under ambient conditions.

2. Results

As mentioned in the Introduction section, we investigated whether the proposed **CAT–1** [28] could actually interact with CO_2 and epoxides. First, peak assignment in the ^1H and ^{13}C NMR spectra was performed through COSY, HSQC, and HMBC experiments (see Supplementary Materials). To determine whether CO_2 can effectively bind to **CAT–1**, **CAT–1** (20 µmol) in 0.5 mL of D_2O was bubbled with 1 bar CO_2 (balloon) at room temperature. As shown in Figure 2a, all ^1H NMR peaks were shifted to downfield. In addition, a newly observed peak appeared at 166 ppm in ^{13}C NMR, as shown in Figure 2b, and is known to be a typical carbamate carbon peak [29]. ^1H and ^{13}C NMR data show that **CAT–1** could readily bind with CO_2 to form an adduct even at room temperature.

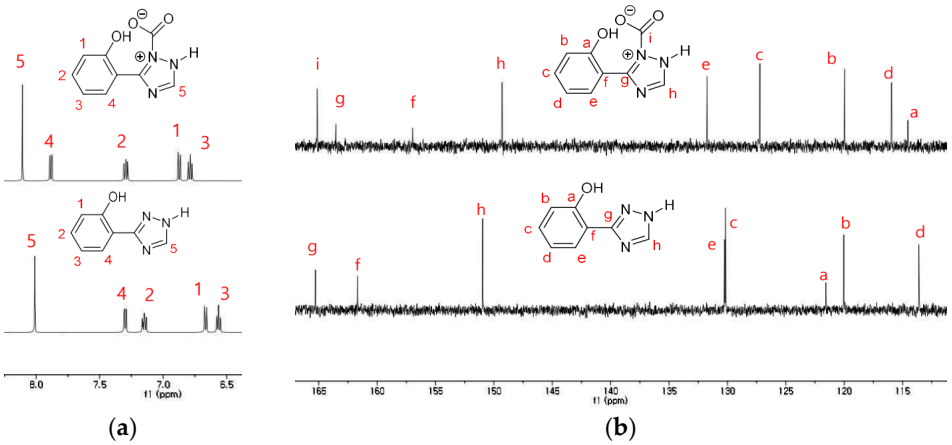

(**a**) (**b**)

Figure 2. (**a**) ^1H NMR spectrum of **CAT–1** before (**bottom**) and after (**top**) bubbling CO_2 in D_2O; (**b**) ^{13}C NMR spectrum of **CAT–1** before (**bottom**) and after (**top**) bubbling CO_2 in D_2O.

Next, the binding pattern of **CAT–1** and epoxides should be investigated. **CAT–1** (20 µmol) was mixed with **1a** (40 µmol) in 0.5 mL of $CDCl_3$ at room temperature. The O–*H* and N–*H* peaks of **CAT–1** in the ^1H NMR spectrum shifted to downfield from 11.2 ppm to 11.4 ppm (see Supplementary Materials). The same trend for the methine proton and methylene protons on the three-membered ring carbons in **1a** was observed. Like CO_2, we found that adducts of **CAT–1** and epoxide could be easily made at room temperature.

Prior to the coupling reaction of CO_2 with epoxides using **CAT–1**, we synthesized five organocatalysts such as 2–(1*H*–pyrazol–3–yl)phenol (**CAT–2**) [30], 2–(1*H*–tetrazol–

5–yl)pyridine (**CAT–3**) [30], 2–(2–methyl–2*H*–tetrazol–5–yl)phenol (**CAT–4**) [31], 2–(1–phenyl–1*H*–imidazol–5–yl)phenol (**CAT–5**) [32], and 2–(2–benzyl–2*H*–tetrazol–5–yl)phenol (**CAT–6**), as shown in Figure 3, to compare the catalytic activity with **CAT–1**.

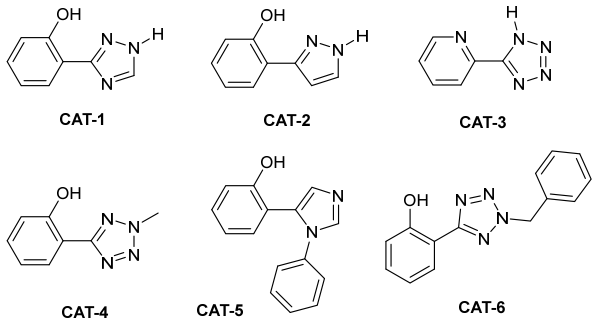

Figure 3. Organocatalysts synthesized and investigated in this study.

The logic of catalyst synthesis is as follows. It is necessary to examine the effect of differences in the number of nitrogen atoms, which act as CO_2-activating sites, on catalytic acidity. Thus, **CAT–2** has one less nitrogen atom in the five-membered ring than **CAT–1**. In **CAT–3**, a pyridine group was introduced instead of a phenol group to investigate the role of phenol in **CAT–1**. Interestingly, the only epoxide-activating site in **CAT–3** is the N–H group, which is known to have weaker HBDs than the O–H group. To investigate the importance of the N–H group present in the five-membered ring of **CAT–1**, we synthesized **CAT–4**, **CAT–5**, and **CAT–6**. They lack N–H groups and have one less HBD than **CAT–1** and **CAT–2**. All compounds were characterized by ^{1}H and ^{13}C NMR spectroscopy (See Supplementary Materials), and single-crystal X-ray diffraction methods were used to confirm the structure of **CAT–6**.

Initially, the coupling of CO_2 with 2–butyloxirane (**1a**) as a substrate as well as a solvent was performed using the organocatalysts given in Figure 3 in the presence of the nucleophilic cocatalyst nBu$_4$NI. The coupling reaction conditions were fixed at 5.0 mol% organocatalyst and 5.0 mol% nBu$_4$NI loadings, a reaction temperature of 25 °C, 1 bar CO_2 (balloon), and a reaction time of 12 h, and the results are summarized in Table 1. As expected, phenol in the presence of nBu$_4$NI showed no catalytic activity for the synthesis of 4–butyl–1,3–dioxolan–2–one (**2a**) (Table 1, entry 1). Binary system 1*H*–1,2,4–triazole/nBu$_4$NI (Table 1, entry 2) and ternary system 1*H*–1,2,4–triazole/phenol/nBu$_4$NI (Table 1, entry 3) showed catalytic activities of 24% and 26%, respectively. This result means that 1*H*–1,2,4–triazole could have much more contribution to the increase in the catalytic activity than phenol. Surprisingly, even at atmospheric CO_2 pressure and ambient temperature, organocatalyst **CAT–1**/nBu$_4$NI easily converted **1a** into **2a,** with a high activity of 96% under the same reaction condition (Table 1, entry 4). The dramatic increase in the catalytic activity for **CAT–1**, a simple form connected between 1*H*–1,2,4–triazole and phenol by a single bond, may originate from the synergistic effect of the sequential existence of a phenol-based strong HBD site, vicinal hydrogen bond acceptor (HBA) site and N–H-based HBD site for epoxide activation, and their vicinal five-membered *N*–heterocycle for CO_2 activation in a single molecule. As shown in entries 5 and 6 of Table 1, **CAT–2**, which has one less nitrogen atom in the five-membered ring, showed similar activity to **CAT–1**; however, the activity of **CAT–3**, which does not contain the –OH group, was found to decrease rapidly. **CAT–4**, **CAT–5**, and **CAT–6**, without N–H groups in the five-membered ring, showed little activity (Table 1, entries 7–9). These data demonstrate that compounds such as **CAT–1**, in which HBD, HBA, and other HBDs are adjacent in order within the molecule, can be used as efficient organocatalysts for the synthesis of cyclic carbonates under ambient conditions.

Table 1. Screening of various catalysts for the coupling of CO_2 to 2–butyloxirane (**1a**) under ambient conditions in the presence of nBu$_4$NI.

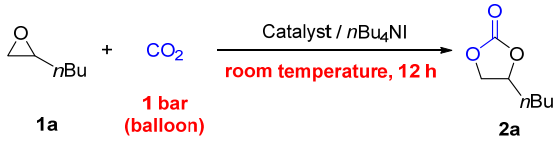

Entry [1]	Catalyst	Conversion (%) [2]	Yield (%) [3]	TON [4]	TOF (h^{-1}) [5]
1	**Phenol**	0	0	0	0
2	**1*H*–1,2,4–triazole**	24	19	4.80	0.40
3	**Phenol+1*H*–1,2,4–triazole**	26	23	5.20	0.43
4	**CAT–1**	96	93	19.2	1.60
5	**CAT–2**	88	87	17.6	1.47
6	**CAT–3**	38	34	7.60	0.63
7	**CAT–4**	3	1	0.60	0.05
8	**CAT–5**	4	2	0.80	0.07
9	**CAT–6**	4	3	0.80	0.07

[1] **1a** (10 mmol), catalyst (0.5 mmol, 5.0 mol%), nBu$_4$NI (0.5 mmol, 5.0 mol%), 25 °C, 1 bar CO_2 (balloon), 12 h, no solvent used. [2] Conversion determined by ^{1}H NMR spectroscopy (see the Supplementary Materials). [3] Isolated yield. [4] TON, turnover number. [5] TOF, turnover frequency (TOF = TON/reaction time (h)).

We then screened a series of nucleophilic cocatalysts, such as nBu$_4$NI, bis(triphenylphosphine)iminium chloride (PPNCl), nBu$_4$NBr, nBu$_4$NCl, DMAP, and KI, in the coupling of **1a** and CO_2 with **CAT–1** (Table 2, entries 1–6). The highest activity was achieved when using **CAT–1** in combination with nBu$_4$NI (Table 2, entry 1). Sterically hindered phosphonium salts were not as effective as nBu$_4$NI (Table 2, entry 2). The catalytic activity decreased in the order I > Br > Cl for tetrabutylammonium salts at 25 °C and 1 bar CO_2 (Table 2, entries 1, 3, and 4). DMAP and KI did not show any catalytic activity (Table 2, entries 5 and 6). Because nBu$_4$NI in conjunction with **CAT–1** showed the highest activity, this was selected as the optimal catalytic system for further investigations and epoxide screening.

Table 2. Screening of various cocatalysts for the coupling of CO_2 to **1a** under ambient conditions using **CAT–1**.

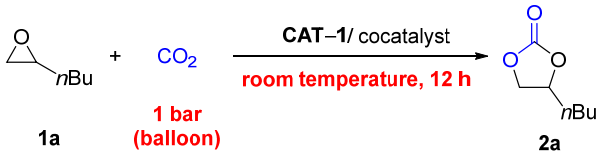

Entry [1]	Cocatalyst	Conversion (%) [2]	Yield (%) [3]	TON [4]	TOF (h^{-1}) [5]
1	**nBu$_4$NI**	96	93	19.2	1.60
2	**PPNCl**	8	7	1.60	0.13
3	**nBu$_4$NBr**	66	61	13.2	1.10
4	**nBu$_4$NCl**	17	16	3.40	0.28
5	**DMAP**	0	0	0	0
6	**KI**	1	1	0.20	0.02

[1] **1a** (10 mmol), **CAT–1** (0.5 mmol, 5.0 mol%), cocatalyst (0.5 mmol, 5.0 mol%), 25 °C, 1 bar CO_2 (balloon), 12 h, no solvent used. [2] Conversion determined by ^{1}H NMR spectroscopy (see the Supplementary Materials). [3] Isolated yield. [4] TON, turnover number. [5] TOF, turnover frequency (TOF = TON/reaction time (h)).

We next investigated the substrate scope using 5.0 mol% **CAT–1** and 5.0 mol% nBu$_4$NI loading at 25 °C and 1 bar CO_2 for 24 h, and the results are shown in Figure 3. The tested substrates included eight epoxides, namely, 2–butyloxirane (**1a**), 2–methyloxirane (**1b**), 2–ethyloxirane (**1c**), 2–phenyloxirane (**1d**), 2–(chloromethyl)oxirane (**1e**), 2–(methoxymethyl)oxirane (**1f**), 2–(*tert*–butoxymethyl)oxirane (**1g**), and 2–(phenoxymethyl)oxirane (**1h**). Generally, the reactivity of epoxides with CO_2 for the synthesis of cyclic carbonates is highly dependent upon the structure of the epoxide. As shown in Figure 4, very high activity for the synthesis of **2a–c** was obtained,

regardless of the type of alkyl chain of epoxides. In addition to this fact, the lower activity of **1d** and **1e** than **1a–c** appears to be due to electronic effects rather than the steric hindrance of the pendant groups on the epoxides. Compared with **2a–c**, **CAT–1**/nBu$_4$NI showed noticeably lower catalytic activities for **2f–h** because of the presence of heteroatoms in the substituents on the epoxide, and these atoms can compete for the formation of H–bonds with **CAT–1**. Steric hindrance (OtBu > OMe) and the electronic effect (OtBu > OPh) also influence the activity of epoxides **1f–1h**. **2h** gave the lowest yield because the phenyl in **1h** may cause iodide attack at the benzylic site, resulting in some yield loss.

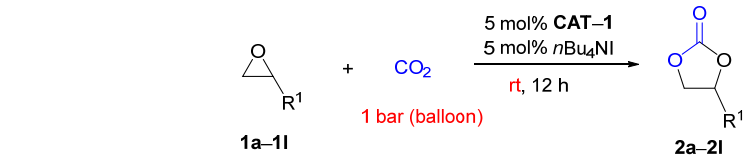

	2a	2b	2c	2d	2e	2f	2g	2h
Conversion (%)	96	96	95	71	87	90	81	62
Yield (%)	93	94	91	70	82	89	77	59
TON	19.2	19.2	19.0	14.2	17.4	18.0	16.2	12.4
TOF (h^{-1})	1.60	1.60	1.58	1.18	1.45	1.50	1.35	1.03

Figure 4. Terminal epoxide scope [33–37].

As shown in Figure 5, we also investigated the synthesis of more challenging cyclic carbonates using 1,2–disubstituted *trans*–2,3–dimethyloxirane (*trans*–**1i**), *cis*–3,6–dioxabicyclo[3.1.0]hexane (*cis*–**1j**), *cis*–6–oxabicyclo[3.1.0]hexane (*cis*–**1k**), and *cis*–7–oxabicyclo[4.1.0]heptane (*cis*–**1l**). Due to the low reactivities of **1i–l**, a high temperature of 70 °C and a high CO_2 pressure of 10 bar were applied. Due to the strain associated with bicyclic epoxides, **1j–l** showed slightly lower reactivity compared with the 1,2–disubstituted epoxide **1i**. The yields of bicyclic carbonates **2k** and **2l** were affected by the ring size of the bicyclic epoxides; **1l,** with a six–membered ring, exhibited lower activity than the five–membered (**1k**) system. All diastereochemically pure epoxides **1i–l** produced the corresponding **2i–l** that maintained their stereochemistry. In addition, no polymeric side products were observed. Thus, the stereochemical retention of cyclic carbonates obtained from the corresponding epoxides indicated that two consecutive S_N2 reactions occurred. This means that there are two inversions of stereochemistry at the carbon atom of the epoxides during the reaction.

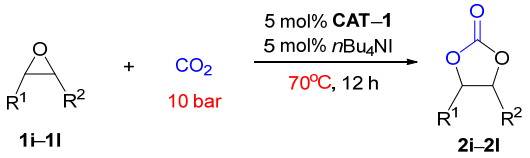

	trans–2i	*cis*–2j	*cis*–2k	*cis*–2l
Conversion (%)	76	47	67	46
Yield (%)	69	44	62	40
TON	15.2	9.4	13.4	9.2
TOF (h^{-1})	1.27	0.78	1.12	0.77
cis*:*trans	> 1:99	> 99:1	> 99:1	> 99:1

Figure 5. Internal epoxide scope [38–41].

As shown in Figure 6, a plausible mechanism for the synthesis of cyclic carbonates from epoxides and CO_2 using **CAT–1** in the presence of the cocatalyst nBu$_4$NI was proposed. This mechanism is similar to that previously proposed for the synthesis of cyclic carbonates using other HBD-based organocatalysts [14]. The epoxide interacts with **CAT–1** via H–bonding to generate intermediate **I**. The insertion of CO_2 into intermediate **I** and the simultaneous nucleophilic ring opening of the epoxide with the iodide anion of the cocatalyst generate carbamate intermediate **II**. The displacement of the iodide in intermediate **II** by the carboxylate anion generates intermediate **III**, followed by the alkoxide attack of the carbamate carbon with concomitant triazole departure. Finally, cyclic carbonates are produced as final products, and intermediate **I** is regenerated.

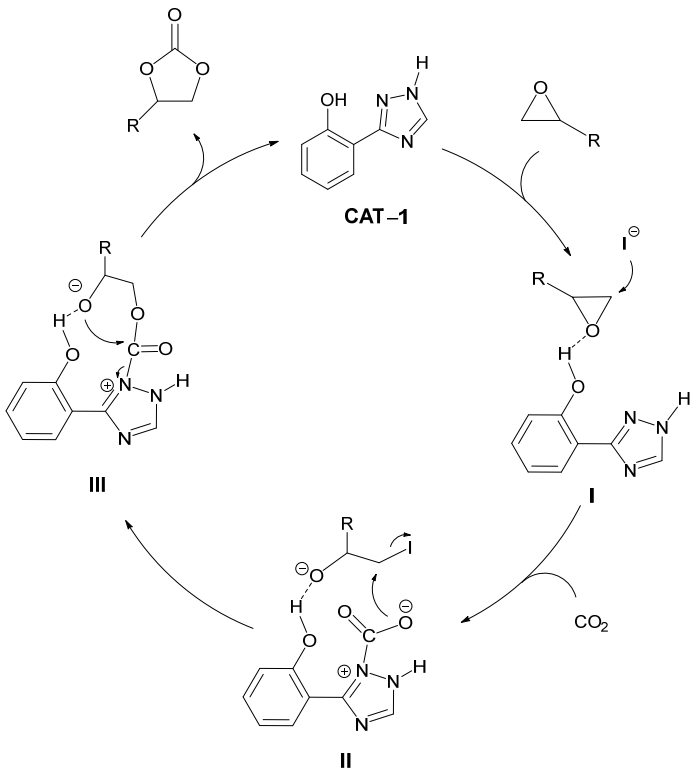

Figure 6. A plausible mechanism for the synthesis of cyclic carbonates from epoxides and CO_2 by using **CAT–1** in the presence of nBu$_4$NI.

3. Materials and Methods

All chemicals were purchased from commercial sources (purity > 95%) and were used as received unless otherwise indicated. Diethyl ether was purified by a Grubbs solvent purification system under a nitrogen atmosphere and stored over activated molecular sieves (4 Å) [42]. Carbon dioxide (99.999%) was used as received without further purification. All epoxides were purified via treatment with calcium hydride to remove residual water. The ^{1}H NMR and ^{13}C NMR spectra were recorded at ambient temperature with a Bruker DPX–500 MHz NMR spectrometer with standard parameters. All chemical shifts are reported in δ units with regard to the residual $CDCl_3$ (δ 7.24 for ^{1}H NMR; δ 77.00 for ^{13}C NMR), DMSO–d_6 (δ 2.50 for ^{1}H NMR; δ 39.52 for ^{13}C NMR) or D_2O (δ 4.79 for ^{1}H NMR). High-resolution mass spectrometry (HRMS) data were acquired using a high-resolution Q–TOF mass spectrometer (ionization mode: ESI).

3.1. Synthesis of Known Compounds

2–(1*H*–1,2,4–Triazol–3–yl)phenol (**CAT–1**) [28], 2–(1*H*–pyrazol–3–yl)phenol (**CAT–2**) [30], 2–(1*H*–tetrazol–5–yl)pyridine (**CAT–3**) [30], 2–(2–methyl–2*H*–tetrazol–5–yl)phenol (**CAT–4**) [31],

2–(1–phenyl–1*H*–imidazol–5–yl)phenol (**CAT–5**) [32] were prepared according to previously published procedures.

*3.2. Synthesis of 2–(2–Benzyl–2H–tetrazol–5–yl)phenol (**CAT–6**)*

Benzyl bromide (1.71 g, 10 mmol) was added to a stirred solution of 2–(1*H*–tetrazol–5–yl)phenol [43] (1.62 g, 10 mmol) in diethyl ether (30 mL). The reaction mixture was stirred at room temperature for 2 h. All volatiles were removed in vacuo, and then the residue was purified via column chromatography using a 1:2 mixture of diethyl ether and hexane as the eluent. **CAT–6** was obtained as a colorless powder with 44% yield (1.1 g). ^{1}H NMR ($CDCl_3$): δ 9.84 (s, 1H, –O*H*), 8.18 (m, 1H), 7.55 (m, 6H), 7.17 (m, 1H), 7.08 (m, 1H), 5.96 (s, 2H, –CH_2Ph). ^{13}C NMR ($CDCl_3$): δ 164.3, 156.3, 132.7, 132.2, 129.2, 129.1, 128.4, 127.4, 120.0, 117.5, 111.1, 57.11. HRMS *m/z* calcd for [$C_{14}H_{12}N_4O$ + H] 253.1089. Found: 253.1084.

3.3. Representative Procedure for the Coupling of Terminal Epoxide and CO_2 at Ambient Condition

Terminal epoxides **1a**–**h** (10 mmol), **CAT–1** (80.6 mg, 0.5 mmol), and *n*Bu_4NI (184.7 mg, 0.5 mmol) were charged in a 20 mL round-bottomed flask with a magnetic stirring bar in a glovebox. A rubber balloon containing approximately 2 L of CO_2 was connected to the flask, and then the reaction vessel was well sealed. The reaction vessel was stirred at 25 °C for 12 h. After 12 h, an aliquot of the reaction mixture was transferred to an NMR tube, and the conversion was determined by ^{1}H NMR spectroscopy. Synthesized cyclic carbonates **2a**–**h** were purified using column chromatography.

3.4. Representative Procedure for the Coupling of Internal Epoxide and CO_2 at Ambient Condition

Internal epoxides *trans*–**1i**, cis–**1j**, cis–**1k** and cis–**1l** (10 mmol), **CAT–1** (80.6 mg, 0.5 mmol), and *n*Bu_4NI (184.7 mg, 0.5 mmol) were charged into a 20 mL stainless steel autoclave with a magnetic stirring bar in a glovebox. The autoclave was pressurized to 10 bar of CO_2 and was heated to 70 °C. After 12 h, the reactor was cooled and vented. An aliquot of the reaction mixture was transferred to an NMR tube, and the conversion and stereochemistry of *trans*–**1i** into *trans*–**2i** was determined via ^{1}H NMR spectroscopy. Synthesized cyclic carbonates **2i**–**l** were purified using column chromatography.

3.5. X-ray Crystallographic Structure Determination

The crystallographic measurement was performed at 293(2) K for **CAT–6** using a Bruker Apex II diffractometer with Mo K_α (λ = 0.71073 Å) radiation. Specimens of suitable quality and size were selected, mounted, and centered on the X-ray beam using a video camera. The structures were solved via direct methods and refined by full-matrix least-squares methods using the SHELXTL program package with anisotropic thermal parameters for all non-hydrogen atoms, resulting in the X-ray crystallographic data of **CAT–6** being obtained in CIF format. Final refinement based on the reflections ($I > 2\sigma(I)$) converged at R_1 = 0.0491, wR_2 = 0.11193, and GOF = 1.010 for **CAT–6**. Further details are given in Table S1 (see the Supplementary Materials). CCDC 1900793 (**CAT–6**) contains the supplementary crystallographic data for this paper. These data can be obtained free of charge from the Cambridge Crystallographic Data Centre.

4. Conclusions

We developed one of the most effective organocatalysts reported to date for the generation of cyclic carbonates via the coupling of epoxides and CO_2 under an ambient temperature and CO_2 pressure. Among our six rationally designed organocatalysts, the solid-state structure for 2–(2–benzyl–2*H*–tetrazol–5–yl)phenol was determined by single-crystal X-ray diffraction analysis. Among the organocatalysts, 2–(1*H*–1,2,4–triazol–3–yl)phenol, which has vicinal –OH and –NH groups as cooperative hydrogen-bond donors and a triazolyl group providing multiple CO_2-activating sites, showed the best catalytic activity for the synthesis of cyclic carbonates in the presence of *n*Bu_4NI as a cocatalyst. The 2–(1*H*–1,2,4–Triazol–3–yl)phenol/*n*Bu_4NI catalytic system was highly effective in the for-

mation of cyclic carbonates from a wide range of terminal epoxides under ambient conditions. This system could convert the internal epoxides at 70 °C and 10 bar CO_2 pressure within 12 h. The cyclic carbonates obtained from the 1,2–disubstituted epoxides showed stereochemical retention due to two consecutive S_N2 reactions.

Supplementary Materials: The following supporting information can be downloaded at: https://www.mdpi.com/article/10.3390/catal14010090/s1, Table S1: List of known compounds [28,30–41]; Table S2: Crystallographic data for **CAT–6**; Figure S1: X-ray structure for 2–(2–benzyl–2*H*–tetrazol–5–yl)phenol(**CAT–6**); Figure S2: ^{1}H NMR spectrum of 2–(1*H*–1,2,4–triazol–3–yl)phenol (**CAT–1**) in $CDCl_3$; Figure S3: ^{1}H NMR spectrum of 2–(1*H*–1,2,4–triazol–3–yl)phenol (**CAT–1**) in D_2O; Figure S4: ^{13}C NMR spectrum of 2–(1*H*–1,2,4–triazol–3–yl)phenol (**CAT–1**) in D_2O; Figure S5: HR-MS spectrum of 2–(1*H*–1,2,4–triazol–3–yl)phenol (**CAT–1**); Figure S6: COSY spectrum of 2–(1*H*–1,2,4–triazol–3–yl)phenol (**CAT–1**) in D_2O; Figure S7: HSQC spectrum of 2–(1*H*–1,2,4–triazol–3–yl)phenol (**CAT–1**) in D_2O; Figure S8: HMBC spectrum of 2–(1*H*–1,2,4–triazol–3–yl)phenol (**CAT–1**) in D_2O; Figure S9: ^{1}H NMR spectrum of **CAT–1** before (bottom) and after (top) bubbling CO_2 in D_2O; Figure S10: ^{13}C NMR spectrum of **CAT–1** before (bottom) and after (top) bubbling CO_2 in D_2O; Figure S11: ^{1}H NMR spectrum of **CAT–1** (bottom), **1a** (middle), and a mixture of **CAT–1** and **1a** (top) in $CDCl_3$. (a) O–*H* and N–*H* peaks in the ^{1}H NMR spectrum of **CAT–1** before (bottom) and after (top) adding **1a** in $CDCl_3$; (b) The methine proton and methylene protons on the three-membered ring carbons in the ^{1}H NMR spectrum of **1a** before (bottom) and after (top) adding **CAT–1** in $CDCl_3$; Figure S12: O–*H* and N–*H* peaks in the ^{1}H NMR spectrum of **CAT–1** before (bottom) and after (top) adding **1a** in $CDCl_3$; Figure S13: The methine proton and methylene protons on the three-membered ring carbons in the ^{1}H NMR spectrum of **1a** before (bottom) and after (top) adding **CAT–1** in $CDCl_3$; Figure S14: ^{1}H NMR spectrum of 2–(1*H*–pyrazol–3–yl)phenol (**CAT–2**) in $CDCl_3$; Figure S15: ^{13}C NMR spectrum of 2–(1*H*–pyrazol–3–yl)phenol (**CAT–2**) in $CDCl_3$; Figure S16: ^{1}H NMR spectrum of 2–(1*H*–tetrazol–5–yl)pyridine (**CAT–3**) in DMSO–d_6; Figure S17: ^{13}C NMR spectrum of 2–(1*H*–tetrazol–5–yl)pyridine (**CAT–3**) in DMSO–d_6; Figure S18: ^{1}H NMR spectrum of 2–(2–methyl–2*H*–tetrazol–5–yl)phenol (**CAT–4**) in $CDCl_3$; Figure S19: ^{13}C NMR spectrum of 2–(2–methyl–2*H*–tetrazol–5–yl)phenol (**CAT–4**) in $CDCl_3$; Figure S20: ^{1}H NMR spectrum of 2–(1–phenyl–1*H*–imidazol–5–yl)phenol (**CAT–5**) in $CDCl_3$; Figure S21: ^{13}C NMR spectrum of 2–(1–phenyl–1*H*–imidazol–5–yl)phenol (**CAT–5**) in $CDCl_3$; Figure S22: ^{1}H NMR spectrum of 2–(2–benzyl–2*H*–tetrazol–5–yl)phenol (**CAT–6**) in $CDCl_3$; Figure S23: ^{13}C NMR spectrum of 2–(2–benzyl–2*H*–tetrazol–5–yl)phenol (**CAT–6**) in $CDCl_3$; Figure S24: HR-MS spectrum of 2–(2–benzyl–2*H*–tetrazol–5–yl)phenol (**CAT–6**); Figure S25: ^{1}H NMR spectrum for an aliquot of the reaction mixture after reaction in Table 1, entry 1; Figure S26: ^{1}H NMR spectrum for an aliquot of the reaction mixture after reaction in Table 1, entry 2; Figure S27: ^{1}H NMR spectrum for an aliquot of the reaction mixture after reaction in Table 1, entry 3; Figure S28: ^{1}H NMR spectrum for an aliquot of the reaction mixture after reaction in Table 1, entry 4; Figure S29: ^{1}H NMR spectrum for an aliquot of the reaction mixture after reaction in Table 1, entry 5; Figure S30: ^{1}H NMR spectrum for an aliquot of the reaction mixture after reaction in Table 1, entry 6; Figure S31: ^{1}H NMR spectrum for an aliquot of the reaction mixture after reaction in Table 1, entry 7; Figure S32: ^{1}H NMR spectrum for an aliquot of the reaction mixture after reaction in Table 1, entry 8; Figure S33: ^{1}H NMR spectrum for an aliquot of the reaction mixture after reaction in Table 1, entry 9; Figure S34: ^{1}H NMR spectrum for an aliquot of the reaction mixture after reaction in Table 2, entry 2; Figure S35: ^{1}H NMR spectrum for an aliquot of the reaction mixture after reaction in Table 2, entry 3; Figure S36: ^{1}H NMR spectrum for an aliquot of the reaction mixture after reaction in Table 2, entry 4; Figure S37: ^{1}H NMR spectrum for an aliquot of the reaction mixture after reaction in Table 2, entry 5; Figure S38: ^{1}H NMR spectrum for an aliquot of the reaction mixture after reaction in Table 2, entry 6; Figure S39: ^{1}H NMR spectrum for an aliquot containing mixtures after reaction for **2b** in Figure 3; Figure S40: ^{1}H NMR spectrum for an aliquot containing mixtures after reaction for **2c** in Figure 3; Figure S41: ^{1}H NMR spectrum for an aliquot containing mixtures after reaction for **2d** in Figure 3; Figure S42: ^{1}H NMR spectrum for an aliquot containing mixtures after reaction for **2e** in Figure 3; Figure S43: ^{1}H NMR spectrum for an aliquot containing mixtures after reaction for **2f** in Figure 3; Figure S44: ^{1}H NMR spectrum for an aliquot containing mixtures after reaction for **2g** in Figure 3; Figure S45: ^{1}H NMR spectrum for an aliquot containing mixtures after reaction for **2h** in Figure 3; Figure S46: ^{1}H NMR spectrum for an aliquot containing mixtures after reaction for *trans*–**2i** in Figure 4; Figure S47: ^{1}H NMR spectrum for an aliquot containing mixtures after reaction for *cis*–**2j** in Figure 4; Figure S48: ^{1}H NMR spectrum for an aliquot containing mixtures after

reaction for *cis*–**2k** in Figure 4; Figure S49: ^{1}H NMR spectrum for an aliquot containing mixtures after reaction for *cis*–**2l** in Figure 4; Figure S50: ^{1}H NMR spectrum of purified 4–butyl–1,3–dioxolan–2–one (**2a**) in $CDCl_3$; Figure S51: ^{13}C NMR spectrum of purified 4–butyl–1,3–dioxolan–2–one (**2a**) in $CDCl_3$; Figure S52: ^{1}H NMR spectrum of purified 4–methyl–1,3–dioxolan–2–one (**2b**) in $CDCl_3$; Figure S53: ^{13}C NMR spectrum of purified 4–methyl–1,3–dioxolan–2–one (**2b**) in $CDCl_3$; Figure S54: ^{1}H NMR spectrum of purified 4–ethyl–1,3–dioxolan–2–one(**2c**) in $CDCl_3$; Figure S55: ^{13}C NMR spectrum of purified 4–ethyl–1,3–dioxolan–2–one(**2c**) in $CDCl_3$; Figure S56: ^{1}H NMR spectrum of purified 4–phenyl–1,3–dioxolan–2–one(**2d**) in $CDCl_3$; Figure S57: ^{13}C NMR spectrum of purified 4–phenyl–1,3–dioxolan–2–one(**2d**) in $CDCl_3$; Figure S58: ^{1}H NMR spectrum of purified 4–(chloromethyl)–1,3–dioxolan–2–one(**2e**) in $CDCl_3$; Figure S59: ^{13}C NMR spectrum of purified 4–(chloromethyl)–1,3–dioxolan–2–one(**2e**) in $CDCl_3$; Figure S60: ^{1}H NMR spectrum of purified 4–(methoxymethyl)–1,3–dioxolan–2–one(**2f**) in $CDCl_3$; Figure S61: ^{13}C NMR spectrum of purified 4–(methoxymethyl)–1,3–dioxolan–2–one(**2f**) in $CDCl_3$; Figure S62: ^{1}H NMR spectrum of purified 4–[(1,1–dimethylethoxy)methyl]–1,3–dioxolan–2–one(**2g**) in $CDCl_3$; Figure S63: ^{13}C NMR spectrum of purified 4–[(1,1–dimethylethoxy)methyl]–1,3–dioxolan–2–one(**2g**) in $CDCl_3$; Figure S64: ^{1}H NMR spectrum of purified 4–(phenoxymethyl)–1,3–dioxolan–2–one(**2h**) in $CDCl_3$; Figure S65: ^{13}C NMR spectrum of purified 4–(phenoxymethyl)–1,3–dioxolan–2–one(**2h**) in $CDCl_3$; Figure S66: ^{1}H NMR spectrum of purified *trans*–4,5–dimethyl–1,3–dioxolan–2–one(*trans*–**2i**) in $CDCl_3$; Figure S67: ^{13}C NMR spectrum of purified *trans*–4,5–dimethyl–1,3–dioxolan–2–one(*trans*–**2i**) in $CDCl_3$; Figure S68: ^{1}H NMR spectrum of purified cis–tetrahydrofuro[3,4–d][1,3]dioxol–2–one(cis–2j) in CDCl3; Figure S69: 13C NMR spectrum of purified cis–tetrahydrofuro[3,4–d][1,3]dioxol–2–one (cis–2j) in CDCl3; Figure S70: 1H NMR spectrum of purified cis–tetrahydro–4H–cyclopenta[d][1,3]dioxol–2–one (cis–2k) in CDCl3; Figure S71: 13C NMR spectrum of purified cis–tetrahydro–4H–cyclopenta[d][1,3]dioxol–2–one(cis–2k) in CDCl3; Figure S72: 1H NMR spectrum of purified cis–hexahydrobenzo[d][1,3]dioxol–2–one (cis–2l) in CDCl3; Figure S73: 13C NMR spectrum of purified cis–hexahydrobenzo[d][1,3]dioxol–2–one(cis–2l) in CDCl3.

Author Contributions: Conceptualization, Y.K. (Yoseph Kim) and Y.K. (Youngjo Kim); Data curation, S.C.; Investigation, Y.S., S.L., S.C. and Y.K. (Yoseph Kim); Supervision, Y.K. (Youngjo Kim); Validation, Y.K. (Yoseph Kim); Writing—original draft, Y.S., S.L. and Y.K. (Yoseph Kim); Writing—review and editing, Y.K. (Youngjo Kim). All authors have read and agreed to the published version of the manuscript.

Funding: This work was supported by the National Research Foundation funded by the Ministry of Science and ICT of Korea (2020R1A2C2006412) and funding for the academic research program of Chungbuk National University in 2022.

Data Availability Statement: The original data are include in the article and Supplementary Materials. Further inquiries can be directly addressed to the corresponding author.

Conflicts of Interest: The authors declare no conflicts of interest.

References

1. Bobbink, F.D.; Van Muyden, A.P.; Dyson, P.J. En route to CO_2-containing renewable materials: Catalytic synthesis of polycarbonates and non-isocyanate polyhydroxyurethanes derived from cyclic carbonates. *Chem. Commun.* **2019**, *55*, 1360–1373. [CrossRef] [PubMed]
2. Song, Q.-W.; Zhou, Z.-H.; He, L.-N. Efficient, selective and sustainable catalysis of carbon dioxide. *Green Chem.* **2017**, *19*, 3707–3728. [CrossRef]
3. Weidlich, T.; Kamenická, B. Utilization of CO_2-available organocatalysts for reactions with industrially important epoxides. *Catalysts* **2022**, *12*, 298. [CrossRef]
4. Martín, C.; Fiorani, G.; Kleij, A.W. Recent advances in the catalytic preparation of cyclic organic carbonates. *ACS Catal.* **2015**, *5*, 1353–1370. [CrossRef]
5. Alves, M.; Grignard, B.; Mereau, R.; Jerome, C.; Tassaing, T.; Detrembleur, C. Organocatalyzed coupling of carbon dioxide with epoxides for the synthesis of cyclic carbonates: Catalyst design and mechanistic studies. *Catal. Sci. Technol.* **2017**, *7*, 2651–2684. [CrossRef]
6. Cokoja, M.; Wilhelm, M.E.; Anthofer, M.H.; Herrmann, W.A.; Kühn, F.E. Synthesis of cyclic carbonates from epoxides and carbon dioxide by using organocatalysts. *ChemSusChem* **2015**, *8*, 2436–2454. [CrossRef] [PubMed]
7. Shaikh, R.R.; Pornpraprom, S.; D'Elia, V. Catalytic strategies for the cycloaddition of pure, diluted, and waste CO_2 to epoxides under ambient conditions. *ACS Catal.* **2018**, *8*, 419–450. [CrossRef]

8. Fiorani, G.; Guo, W.; Kleij, A.W. Sustainable conversion of carbon dioxide: The advent of organocatalysis. *Green Chem.* **2015**, *17*, 1375–1389. [CrossRef]
9. Yingcharoen, P.; Kongtes, C.; Arayachukiat, S.; Suvarnapunya, K.; Vummaleti, S.V.C.; Wannakao, S.; Cavallo, L.; Poater, A.; D'Elia, V. Assessing the pKa–dependent activity of hydroxyl hydrogen bond donors in the organocatalyzed cycloaddition of carbon dioxide to epoxides: Experimental and theoretical study. *Adv. Synth. Catal.* **2019**, *361*, 366–373. [CrossRef]
10. Arayachukiat, S.; Kongtes, C.; Barthel, A.; Vummaleti, S.V.C.; Poater, A.; Wannakao, S.; Cavallo, L.; D'Elia, V. Ascorbic acid as a bifunctional hydrogen bond donor for the Synthesis of cyclic carbonates from CO_2 under ambient conditions. *ACS Sustain. Chem. Eng.* **2017**, *5*, 6392–6397. [CrossRef]
11. Wang, L.; Zhang, G.; Kodama, K.; Hirose, T. An efficient metal- and solvent-free organocatalytic system for chemical fixation of CO_2 into cyclic carbonates under mild conditions. *Green Chem.* **2016**, *18*, 1229–1233. [CrossRef]
12. Hardman-Baldwin, A.M.; Mattson, A.E. Silanediol-catalyzed carbon dioxide fixation. *ChemSusChem* **2014**, *7*, 3275–3278. [CrossRef] [PubMed]
13. Sperandio, C.; Rodriguez, J.; Quintard, A. Organocatalytic carbon dioxide fixation to epoxides by perfluorinated 1,3,5-triols catalysts. *Org. Biomol. Chem.* **2020**, *18*, 2637–2640. [CrossRef] [PubMed]
14. Hong, M.; Kim, Y.; Kim, H.; Cho, H.J.; Baik, M.-H.; Kim, Y. Scorpionate catalysts for coupling CO_2 and epoxides to cyclic carbonates: A rational design approach for organocatalysts. *J. Org. Chem.* **2018**, *83*, 9370–9380. [CrossRef]
15. Liu, N.; Xie, Y.-F.; Wang, C.; Li, S.-J.; Wei, D.; Li, M.; Dai, B. Cooperative multifunctional organocatalysts for ambient conversion of carbon dioxide into cyclic carbonates. *ACS Catal.* **2018**, *8*, 9945–9957. [CrossRef]
16. Zhou, H.; Wang, G.-X.; Zhang, W.-Z.; Lu, X.-B. CO_2 adducts of phosphorus ylides: Highly active organocatalysts for carbon dioxide transformation. *ACS Catal.* **2015**, *5*, 6773–6779. [CrossRef]
17. Wu, X.; Chen, C.; Guo, Z.; North, M.; Whitwood, A.C. Metal- and halide-free catalyst for the synthesis of cyclic carbonates from epoxides and carbon dioxide. *ACS Catal.* **2019**, *9*, 1895–1906. [CrossRef]
18. Wang, J.; Zhang, Y. Boronic acids as hydrogen bond donor catalysts for efficient conversion of CO_2 into organic carbonate in water. *ACS Catal.* **2016**, *6*, 4871–4876. [CrossRef]
19. Gennen, S.; Alves, M.; Mereau, R.; Tassaing, T.; Gilbert, B.; Detrembleur, C.; Jerome, C.; Grignard, B. Fluorinated alcohols as activators for the solvent–free chemical fixation of carbon dioxide into epoxides. *ChemSusChem* **2015**, *8*, 1845–1849. [CrossRef]
20. Martinez–Rodriguez, L.; Garmilla, J.O.; Kleij, A.W. Cavitand-based polyphenols as highly reactive organocatalysts for the coupling of carbon dioxide and oxiranes. *ChemSusChem* **2016**, *9*, 749–755. [CrossRef] [PubMed]
21. Sopena, S.; Fiorani, G.; Martin, C.; Kleij, A.W. Highly efficient organocatalyzed conversion of oxiranes and CO_2 into organic carbonates. *ChemSusChem* **2015**, *8*, 3248–3254. [CrossRef] [PubMed]
22. Alves, M.; Grignard, B.; Gennen, S.; Detrembleur, C.; Jerome, C.; Tassaing, T. Organocatalytic synthesis of bio-based cyclic carbonates from CO_2 and vegetable oils. *RSC Adv.* **2015**, *5*, 53629–53636. [CrossRef]
23. Whiteoak, C.J.; Henseler, A.H.; Ayats, C.; Kleij, A.W.; Pericas, M.A. Conversion of oxiranes and CO_2 to organic cyclic carbonates using a recyclable, bifunctional polystyrene-supported organocatalysts. *Green Chem.* **2014**, *16*, 1552–1559. [CrossRef]
24. Whiteoak, C.J.; Nova, A.; Maseras, F.; Kleij, A.W. Merging sustainability with organocatalysis in the formation of organic carbonates by using CO_2 as a feedstock. *ChemSusChem* **2012**, *5*, 2032–2038. [CrossRef] [PubMed]
25. Wang, J.-Q.; Sun, J.; Cheng, W.-G.; Dong, K.; Zhang, X.-P.; Zhang, S.-J. Experimental and theoretical studies on hydrogen bond-promoted fixation of carbon dioxide and epoxides in cyclic carbonates. *Phys. Chem. Chem. Phys.* **2012**, *14*, 11021–11026. [CrossRef]
26. Takaishi, K.; Okuyama, T.; Kadosaki, S.; Uchiyama, M.; Ema, T. Hemisquaramide tweezers as organocatalysts: Synthesis of cyclic carbonates from epoxides and CO_2. *Org. Lett.* **2019**, *21*, 1397–1401. [CrossRef]
27. Fan, Y.; Tiffner, M.; Schörgenhumer, J.; Robiette, R.; Waser, M.; Kass, S.R. Synthesis of cyclic organic carbonates using atmospheric pressure CO_2 and charge–containing thiourea catalysts. *J. Org. Chem.* **2018**, *83*, 9991–10000. [CrossRef] [PubMed]
28. Pagacz-Kostrzewa, M.; Saldyka, M.; Wierzejewska, M.; Khomenko, D.M.; Doroschuk, R.O. Theoretical DFT and matrix isolation FT IR studies of 2-(1,2,4-triazolyl)phenol isomers. *Chem. Phys. Lett.* **2016**, *657*, 156–161. [CrossRef]
29. Wada, S.; Kushida, T.; Itagaki, H.; Shibue, T.; Kadowaki, H.; Arakawa, J.; Furukawa, Y. ^{13}C NMR study on carbamate hydrolysis reactions in aqueous amine/CO_2 solutions. *Int. J. Greenh. Gas Control* **2021**, *104*, 103175. [CrossRef]
30. Kumar, S.; Jaller, D.; Patel, B.; LaLonde, J.M.; DuHadaway, J.B.; Malachowski, W.P.; Prendergast, G.C.; Muller, A.J. Structure based development of phenylimidazole-derived inhibitors of indoleamine 2,3-dioxygenase. *J. Med. Chem.* **2008**, *51*, 4968–4977. [CrossRef]
31. Padwa, A.; Nahm, S.; Sato, E. Intramolecular 1,3-dipolar cycloaddition reactions of alkenyl-substituted nitrile imines. *J. Org. Chem.* **1978**, *43*, 1664–1671. [CrossRef]
32. Castro-Osma, J.A.; Martinez, J.; de la Cruz-Martinez, F.; Caballero, M.P.; Fernandez-Baeza, J.; Rodriguez-Lopez, J.; Otero, A.; Lara-Sanchez, A.; Tejeda, J. Development of hydroxy-containing imidazole organocatalysts for CO_2 fixation into cyclic carbonates. *Catal. Sci. Technol.* **2018**, *8*, 1981–1987. [CrossRef]
33. Whiteoak, C.J.; Kielland, N.; Laserna, V.; Escudero-Adán, E.C.; Martin, E.; Kleij, A.W. A powerful aluminum catalyst for the synthesis of highly functional organic carbonates. *J. Am. Chem. Soc.* **2013**, *135*, 1228–1231. [CrossRef] [PubMed]
34. Cho, W.; Shin, M.S.; Hwang, S.; Kim, H.; Kim, M.; Kim, J.G.; Kim, Y. Tertiary amines: A new class of highly efficient organocatalysts for CO_2 fixations. *J. Ind. Eng. Chem.* **2016**, *44*, 210–215. [CrossRef]

35. Li, P.-Z.; Wang, X.-J.; Liu, J.; Lim, J.S.; Zou, R.; Zhao, Y. A triazole-containing metal-organic framework as a highly effective and substrate size-dependent catalyst for CO_2 conversion. *J. Am. Chem. Soc.* **2016**, *138*, 2142–2145. [CrossRef]
36. Paddock, R.L.; Nguyen, S.T. Chemical CO_2 fixation: Cr(III) salen complexes as highly efficient catalysts for the coupling of CO_2 and epoxides. *J. Am. Chem. Soc.* **2001**, *123*, 11498–11499. [CrossRef] [PubMed]
37. Kim, H.; Choi, S.H.; Ahn, D.; Kim, Y.; Ryu, J.Y.; Lee, J.; Kim, Y. Facile synthesis of a dimeric titanium(IV) complex with terminal Ti=O moieties and its application as a catalyst for the cycloaddition reaction of CO_2 to epoxides. *RSC Adv.* **2016**, *6*, 97800–97807. [CrossRef]
38. Stewart, J.A.; Drexel, R.; Arstad, B.; Reubsaet, E.; Weckhuysen, B.M.; Bruijnincx, P.C.A. Homogeneous and heterogenized masked N-heterocyclic carbenes for bio-based cyclic carbonate synthesis. *Green Chem.* **2016**, *18*, 1605–1618. [CrossRef]
39. Jose, T.; Canellas, S.; Pericas, M.A.; Kleij, A.W. Polystyrene-supported bifunctional resorcinarenes as cheap, metal-free and recyclable catalysts for epoxides/CO_2 coupling reactions. *Green Chem.* **2017**, *19*, 5488–5493. [CrossRef]
40. Saptal, V.B.; Nanda, B.; Parida, K.M.; Bhanage, B.M. Fabrication of amine and zirconia on MCM-41 as acid-base catlysts for the fixation of carbon dioxide. *ChemCatChem* **2017**, *9*, 4105–4111. [CrossRef]
41. Zheng, X.; Luo, S.; Zhang, L.; Cheng, J.-P. Magnetic nanoparticle supported ionic liquid catalysts for CO_2 cycloaddition reactions. *Green Chem.* **2009**, *11*, 455–458. [CrossRef]
42. Pangborn, A.B.; Giardello, M.A.; Grubbs, R.H.; Rosen, R.K.; Timmers, F.J. Safe and convenient procedure for solvent purification. *Organometallics* **1996**, *15*, 1518–1520. [CrossRef]
43. Shelkar, R.; Singh, A.; Nagarkar, J. Amberlyst-15 catalyzed synthesis of 5-substituted 1-*H*-tetrazole via [3+2] cycloaddition of nitriles and sodium azide. *Tetrahedron Lett.* **2013**, *54*, 106–109. [CrossRef]